104 (2025) 104939

Contents lists available at ScienceDirect

Poultry Science

journal homepage: www.elsevier.com/locate/psj

Dichlorvos poisoning caused chicken cerebellar autophagy and changes of Caecal microflora

Juan Chen [a,1], Yun Zhang [c,1], Chenxi Jiang [a], Shupeng Chen [b], Yulan Zhao [a], Xiaona Gao [a], Xiaoquan Guo [a], Guoliang Hu [a], Pei Liu [a], Huibo Jin [a], Ying Zhang [a], Salma Mbarouk Omar [a], Lin Li [a], Gen Wan [a], Ping Liu [a,*]

[a] Jiangxi Provincial Key Laboratory for Animal Health, Institute of Animal Population Health, College of Animal Science and Technology, Jiangxi Agricultural University, Nanchang 330045, PR China
[b] Jiangxi Agricultural Engineering Vocational college, Zhangshu, Jiangxi 331200, PR China
[c] Huaihua City Maternal and Child Health Care Hospital, Huaihua, Hunan 418000, PR China

ARTICLE INFO

Keywords:
Dichlorvos
Broiler
Cerebellum
Autophagy
Caecal microflora

ABSTRACT

In order to explore the effects of acute dichlorvos exposure on cerebellar autophagy and cecal microbes in broilers and to analyze the relationship between autophagy-related genes and cecal microbes. Broilers were randomly divided into three groups (with 16 broilers in each group)and respectively given distilled water and dichlorvos (2.48 mg / kg, 11.3 mg / kg). The cecal contents and cerebellum samples were collected after poisoning symptoms of broilers, and the antioxidant indexes such as SOD and CAT in cerebellum were detected. Hematoxylin-eosin (HE) staining of cerebellum and cecum, and immunofluorescence sections of cerebellum LC3 were made. RT-PCR and western blot were used to detect the expression of oxidative stress and autophagy-related genes in cerebellar tissue. The cecal contents were analyzed by 16S rRNA high-throughput sequencing, and then the correlation between the expression of autophagy-related genes and the abundance of intestinal microbes was analyzed. It was concluded that dichlorvos exposure destroyed the normal morphological structure of the cerebellum and cecum in broilers, which induced oxidative stress and autophagy in the cerebellum of broilers, reduced the diversity of cecal microorganisms, and destroyed the steady state of the cecal microbial structure. In addition, The changes of mRNA expression of autophagy-related genes is related to some specific bacteria. In summary, this study found that dichlorone exposure can cause cerebellar oxidative stress and autophagy, and the mechanism of cerebellar injury in broilers is linked to cecal microbiota changes, potentially offering a new direction for researching dichlorone's pathogenic mechanism.

Introduction

Dichlorvos (DDVP) is an organophosphorus pesticide commonly used in agricultural production. Due to its high efficiency, low price and availability, it has been widely used since 1961 as crop protectants and general public health insecticides(Coggon, 2002). Dichlorvos is volatile, so it is easy for humans or livestock to be exposed to dichlorvos through air, water or food and other channels, which can be absorbed by the body and lead to poisoning. The main toxicological effect of dichlorvos is that it inhibits the activity of cholinesterase (AChE), which directly acts as an anticholinesterase and causes excessive accumulation of acetylcholine, leading to acute poisoning (Kwong, 2002; Rusyniak and Nanagas, 2004). Although there is a long history of research on the neurotoxic effects of organophosphorus pesticides, there is relatively little information about the mechanism of action except for the inhibitory effect on AChE. In recent studies, dichlorvos has been found to be neurotoxic. It causes oxidative stress in rat tissues and autophagy in mouse cardiomyocytes. Moreover, in a study on cowpea beetles, the toxic effects of dichlorvos were found to be closely related to the intestinal flora (Akami et al., 2019; Antonijevic et al., 2018; Ben et al., 2023; Bui-Nguyen et al., 2015; Dwivedi et al., 2014).

Oxidative stress has been recognized as a common pathway in toxic diseases (Yang et al., 2018). Dichlorvos has been shown in numerous studies to induce oxidative stress in rats (Antonijevic et al., 2018;

* Corresponding author.
E-mail address: Pingliujx@163.com (P. Liu).
[1] These authors contributed equally to this study and share first authorship.

https://doi.org/10.1016/j.psj.2025.104939
Received 11 January 2025; Accepted 21 February 2025
Available online 21 February 2025

Dwivedi et al., 2014). And the large amount of ros in oxidative stress is also an early inducer of autophagy, and can induce autophagy by regulating the activity of mTOR (Borodkina et al., 2016). Recent studies have shown that dichlorvos can cause autophagy in cardiomyocytes (Ben et al., 2023), the studies focusing on the toxicity mechanisms of dichlorvos on cells other than neuronal cells are relatively few, and no relevant studies on oxidative stress or cellular autophagy in cerebellar tissues using dichlorvos-exposed broiler were reviewed at the time of writing this thesis.

In recent years, the importance of intestinal flora in biological functions has provided a way for the study of many diseases (Borodkina et al., 2016; Li et al., 2019; Zhang et al., 2020). The effects of poisoning on intestinal flora have attracted great attention of researchers, and the changes of intestinal flora may provide a new perspective for the mechanism of poisoning. Various toxicants have been found to cause disturbances in the intestinal flora, for example, monovalent thallium exposure reduced the alpha diversity of bacteria in the intestine and feces of mice (Li et al., 2023); aflatoxin B1 reduced the digestive, absorptive and antioxidant capacity of the intestine and increased the relative abundance of intestinal pathogenic bacteria in pregnant and lactating rats (Li et al., 2023; Wu et al., 2023); methamphetamine exposure altered the alpha and beta diversity of the intestinal microbiota in BALB/c mice (Chen et al., 2021). Therefore, an in-depth exploration and understanding of the changes in intestinal flora is of critical importance to elucidate the potential mechanism of action of dichlorvos. The question of whether significant and observable changes occur in the intestinal flora structure of broiler chickens after exposure to dichlorvos is worthy of in-depth investigation.

In summary, dichlorvos has not been adequately studied in broiler cerebellar autophagy and oxidative stress, and intestinal flora. Our previous studies on the toxicity of chicken brain, cerebellum, and brain stem have found that damage to the cerebellum is the most serious (Huang et al., 2022). Immediately following the results of previous research, we consider the most serious damage of the cerebellum in a subsequent study of damage mechanism, and damage mechanism is probably associated with the gut microbes, which may provide a new research direction for the pathogenic mechanism of dichlorvos.

Materials and methods

Experimental animals and experimental design

Forty-eight healthy 40-day-old white-feathered broilers with an average body weight of 1.1 to 1.5kg were purchased from a meat farm in Nanchang, Jiangxi, China. The forty-eight 40-day-old male white-feathered broilers were randomly divided into three groups: the control group (Con), low-dose group (Low) and high-dose group (High), with 16 broilers in each group. During the experiment, broilers were fed twice a day in a well-ventilated room with a temperature of 20-25°C and humidity of 55 %-60 %. Each broiler had free access to food and water. The rations were standard fattening chicken rations purchased from Jiangxi Chia Tai Feed Co., Ltd. (Jiangxi, China), and the drinking water was pure tap water. The previous research results in our laboratory confirmed that the LD_{50} and LD_{100} of dichlorvos for broilers were 6.2 mg/kg and 11.3 mg/kg respectively, which were basically consistent with the research results in the study by Al-Zubaidy et al and the study by F.K. Mohammad et al (Al-Zubaidy et al., 2011; Mohammad et al., 2008). In our experiment, two-fifths of dichlorvos concentration of LD_{50} was used as the challenge dose of the low-dose group, namely 2.48 mg/kg b.w. Dichlorvos concentration of LD_{100} was taken as the challenge dose of the high-dose group, namely 11.3 mg/kg b.w. The selection of the two challenge doses was in accordance with the experimental dose design principle of acute poisoning. 77.5 % dichlorvos was diluted to 0.1 % solution with distilled water on the day of experiment. The broilers in the control group were fed distilled water. Experimental broilers in the low-dose group were given dichlorvos 2.48 mg/kg. The broilers in the high-dose group were given dichlorvos 11.3 mg/kg.All subsequent animal experiments were conducted with at least six biological replicates.

Sample collection

Samples were collected from broilers in both high-dose group and low-dose group-after obvious symptoms of poisoning. Broilers in Low showed the most obvious poisoning symptoms in 4 to 6 h after challenge. Samples of broilers in Low were collected when the poisoning symptoms were obvious. Broilers in High showed acute poisoning symptoms in 15 to 60 min until death. Samples were collected immediately after death of broilers in High. Before challenge, each broiler was fasted for 12 h and water was forbidden for 6 h. After obvious symptoms of poisoning, the caecum, caecum contents and cerebellum were collected and placed in a sterile 1.5 mL EP tube. After being frozen in liquid nitrogen, they were stored in a cryogenic refrigerator at -80 °C. The cecum and cerebellum were rinsed and fixed in sectioning fixative for making pathological sections.

Histopathological examination

The fixed cerebellum and cecum were rinsed, dehydrated, made transparent and then waxed. The paraformaldehyde-fixed samples were embedded in paraffin and stained with hematoxylin and eosin. The histological slides were then examined by light microscopy.

Measurement of biomarkers of oxidative stress

The 0.5-1 g cerebellar tissue blocks were weighed and put into 2 mL grinding tubes filled with pre-cooled normal saline. Three sterile zirconia grinding beads were added to each tube and ground in an automatic homogenizer for 1 min. Then the grinding tubes containing tissue homogenate were moved to a frozen centrifuge at 4 °C for 3500 r/min and centrifuged for 10 min to separate the supernatant. Then, according to the instructions of the manufacturer of Beijing Huaying Institute of Biotechnology (Beijing, China), the separated supernatant was used to determine SOD, MDA, CAT and T-AOC.

Real-time quantitative PCR

RNA extraction, cDNA synthesis and q-PCR were performed following a previous description (Zhao et al., 2020). Total RNA was isolated using TRIzol reagent (Invitrogen, Burlington, ON, Canada) according to the manufacturer's protocol. We used a Nano Photometer1 spectrophotometer (IMPLEN, CA, USA) to determine RNA purity. The amount of RNA in each sample was quantified with 20 ng cDNA which was synthesized using a TransScript One-Step gDNA Removal and cDNA Synthesis SuperMix reagent kit (TransGen Biotech, Beijing, China) according to the manufacturer's instructions. Then, it was stored at 20 °C for fluorescent quantitation using SYBR Green qRT-PCR. Gene-specific primers for all genes were designed using Primer Premier software (PREMIER Biosoft International, CA, USA). The Glyceraldehyde-3-phosphate dehydrogenase (GAPDH) housekeeping gene was used as an internal reference, and the primer sequences are specified in Table 1. The qPCR profile was as follows: 95 °C for 10 min, 40 cycles at 95 °C for 15 s, 60 °C for 60 s and extension at 95 °C for 15 s. All reactions were carried out using a Light Cycler 96 RT-PCR machine. The data were analyzed by the $2^{-\Delta\Delta Ct}$ method.

Western blotting

Western blotting was performed following a previous description (Zhao et al., 2021). Cerebellum tissues were homogenized in a buffer. The proteins were extracted using a protein extraction kit (Wuhan Seville Biological Technology Co., Ltd, Wuhan, Hubei, China) according

Table 1
Primer sequences

Gene	GenBank Number	Primer sequence (5′-3′)
Nrf2	MN416129.1	R: GCTTTCTCCCGCTCTTTCTG
		F: ATCACCTCTGCACCGAA
HO-1	X56201.1	R: CATCCTGCTTGTCCTCTCAC
		F: CTTCGCACA AGGAGTGTTAAC
SOD-1	NM_205064.1	R: CTAAACGAGGTCCAGCATT
		F: AGGAGTGGCAGAAGTAGAA
CAT	NM_001031215.2	R: GGCTATGGATGAAGGATGG
		F: CACTGTTGCTGGAGAATCT
GCLC	XM_040666478.1	R: TCCTTTATTAGGTGCTCGTAG
		F: TCTGTAGATGATCGAACGC
GCLM	NM_001007953.1	R: TGCATGATATAGCCTTTGGAC
		F: GCTGCTAACTCACAATGACC
GST	L15386.1	R: ATGTCCGTGGTCCTTCAA
		F: CAGAGCCATCCTCAACTAC
NQO1	NM_001277621.1	R: GCCATCTCCATCTCGTAGACA
		F: CCCTCAAGAACCCCGAGT
Beclin1	NC_006114.4	R: TTATTGTCCCAGAAGAACCTCAG
		F: CGTATGGCAACCACTCGTATT
Atg5	XM_001006409.1	R: GCCGAGGAAGGGCTGTATT
		F: AGAGATGTGTGGTTTGGACGC
LC3-A	AW240014.1	R: ATTCCAACCTGTCCCTCA
		F: TTACACCCATATCAGATTCTTG
LC3-B	AW240014.1	R: AAGCCTTGTGAACGAGAT
		F: AGTGAAGTGTAGCAGGATGA
P62	NC_006100.4	R: CAGAGGCATGTAGTTTCGGC
		F: GACCCAGCCAAGACTACCAT
GAPDH	NM_204305	R: CGGCAGGTCAGGTCAACAACAG
		F: GCCATCACAGCCACACAGAAGA

to the manufacturer's instructions. After protein concentration determination by the BCA method, 20 μg protein was transferred to PVDF membranes. Non-specific binding sites were blocked with 5 % skim milk at room temperature for 2 h and incubated overnight at 4 °C with appropriate concentrations of specific antibodies (Wanleibio Co., Ltd, Shenyang, Liaoning, China). After washing, HRP-labelled goat anti-rabbit IgG (High + Low) was incubated at 37 °C for 40 min. Finally, signals were detected using enhanced chemiluminescence kits (Vazyme Biotech Co., Ltd, Nanjing, Jiangsu, China). Protein immunoreactive bands were photographed. Twelve samples were detected, and representative results are shown.

Immunofluorescence of the cerebellum

The whole cerebellum was dissected and transferred immediately into silver paper. The silver paper was snap-frozen by putting above liquid nitrogen for 60 s, and then the completely frozen brain tissues were embedded with OCT compound. Frozen sections (8 μm) were placed at room temperature for 5 min, fixed in 4 % neutral paraformaldehyde for 10 min, blocked with 3 % bovine serum and then incubated with primary antibody overnight at 4 °C. Concentration of LC3 antibody was diluted to 1:4000. The 4′,6-diamidino-2-phenylindole (DAPI) was used as a marker for cell nuclei.

16S rRNA MiSeq sequencing and bioinformatics analysis

Firstly, genomic DNA was extracted, and total DNA was extracted according to previous reports (Ruan et al., 2019). Then 16S rRNA was amplified and sequenced. QIIME and R packages were used to perform sequence analysis. To assess the microbial alpha diversity in a single host, OTU tables were made and sparse curves were generated based on observed species measurements. The α-diversity index, including calculations by ACE, Simpson, Chao1 and Shannon methods, were used to reflect the diversity and richness of communities in different samples. The β-diversity of species differences between different samples was calculated using a weighted Bray-Curtis distance matrix and visualized by principal Coordinate analysis (PCoA). Venn diagrams were drawn using the R software package VennDiagram, which visually shows the number of OTUs shared and uniqueness between different groups. QIIME software was used to draw comparison maps for different levels of species composition analysis. Wilcoxon test was used to calculate the differences between the two groups at phylum level and genus level. Phylogenetic survey (PICRUST) was performed on communities by reconstructing unobserved states to predict the presence of gene families, which were then compared with the Kyoto Encyclopedia of Genes and Genomes (KEGG) database to estimate the predicted genes and their respective functions.

Statistical analysis

SPSS 26.0 software (SPSS Inc., Chicago, IL, USA) was used to perform statistical analysis. All results were expressed in the format of mean ± SE. Comparisons between groups were conducted using ANOVA and T-tests. The results with $P<0.05$ were considered to be significant, and results with $P<0.01$ were considered to be very significant. GraphPad Prism 5.0 (GraphPad Software Inc., San Diego, California, USA) was used to make plots. Image processing software ImageJ (National Institutes of Health, Maryland, USA) was used to annotate images. Relationships between intestinal microbiota and autophagy-related gene expression were analyzed based on Pearson's correlation measures using the R software.

Result

Effects of DDVP on cerebellum and cecum histopathological changes in broilers

Fig. 1(a) shows that compared with Con, chicken cerebellum in Low and High showed obvious pathological injury, the visible cerebellum groove spacing, obvious morphological changes in the glial cells, apparent deformation or cavity formation in purkinje cells, granular cell shrinkage and deformation. With the increase in dichlorvos dose, the cerebellar lesion severity became more serious. Fig. 1(b) shows that compared with Con, chicken caecum in Low and High showed obvious pathological injury, significant muscular thickening, shortened or broken intestinal villi, atrophy of intestinal glands, and reduced goblet cell number.

Effects of DDVP exposure on oxidative stress in broilers

As shown in Fig. 2, compared with Con, the activities of SOD and T-AOC in Low and High were significantly increased ($P<0.05$ or $P<0.01$). The content of MDA in the two groups was also significantly higher than that in the control group ($P<0.01$). There was no statistically significant difference in CAT activity between the two groups ($P>0.05$). The results of cerebellar antioxidant gene mRNA expression showed that the mRNA expression levels of Nrf2, HO-1, SOD-1, CAT, GSH, GCLC, GCLM and NQO1 in the low-dose group were significantly higher than those in the control group. The mRNA expression levels of SOD-1, GSH, GCLC, GCLM and NQO1 in the two dose groups were also significantly up-regulated compared with the control group ($P<0.05$ or $P<0.01$). The mRNA expression levels of Nrf2, HO-1 and CAT showed an upward trend, but the difference was not statistically significant ($P>0.05$).

Effects of dichlorvos on cerebellar autophagy in broilers

The mRNA expression of cerebellar autophagy-related genes in experimental broilers is shown in Fig. 3(a). Compared with the control group, the mRNA expression levels of LC3-A, LC3-B and Atg5 in Low were significantly up-regulated ($P<0.001$ or $P<0.01$). Beclin1 mRNA expression showed an upward trend, but the difference was not statistically significant ($P>0.05$). The mRNA expression levels of LC3-A, LC3-B and Beclin1 in High were significantly up-regulated ($P<0.05$ or

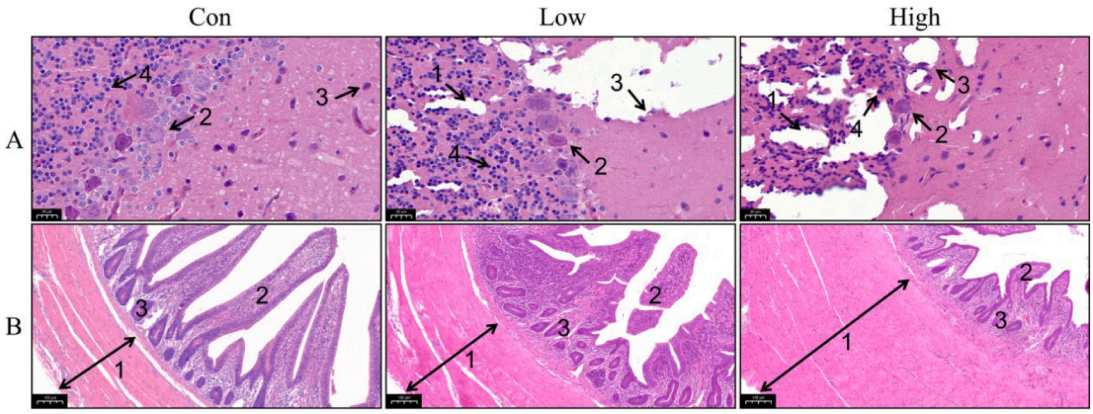

Fig. 1. Histopathological observation of cerebellum (A) and caecum (B) after dichlorvos exposure (200 ×).
A: 1. Cerebellar sulcus; 2. Tissue vacuole; 3. Purkinje cells; 4. Glial cells; 5. Granulosa cell. B: 1. Thickness of muscular layer; 2 Intestinal villi; 3. Large adenomas.

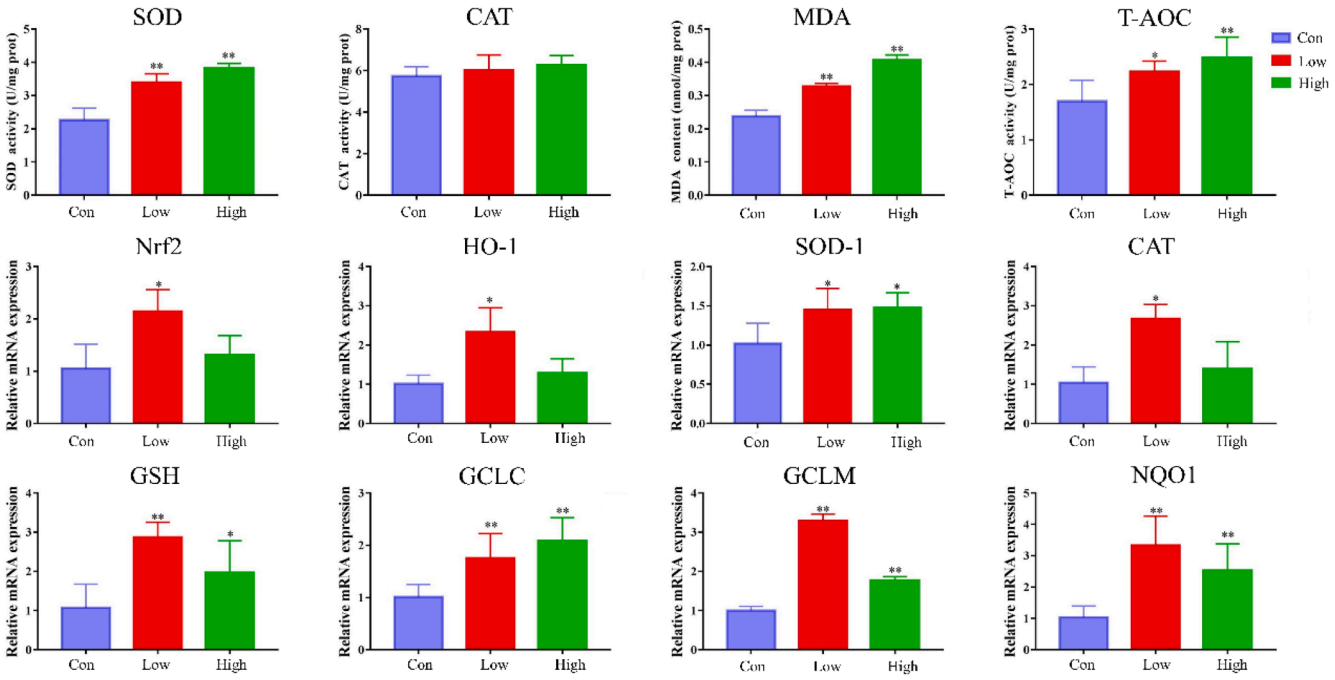

Fig. 2. Effects of dichlorvos on antioxidant markers in cerebellum.
(*:$P<0.05$,**:$P<0.01$)

$P<0.01$), whereas Agt5 mRNA expression did not show statistically significant difference ($P>0.05$). In addition, compared with Con, the P62 mRNA expression level in High was significantly down-regulated ($P<0.05$); the mTOR mRNA expression level was significantly down-regulated in both Low and High ($P<0.05$ or $P<0.01$).

The expression level of cerebellar autophagy-related protein is shown in Fig. 3(b). Compared with Con, the expression level of LC3-II/LC3-I protein in Low was significantly up-regulated ($P<0.01$), and Beclin1 protein in High was significantly increased ($P<0.05$). In addition, compared with Con, there was no statistically significant difference in P62 protein expression between the other two groups ($P>0.05$).

Fig. 3(c) shows the positive expression of LC3 in the cerebellar cytoplasm detected by the immunofluorescence method. The nucleus was labeled with DAPI and the label was blue. The LC3 protein in the cytoplasm was stained red by the antibody. We found that compared with Con, the positive expression level of LC3 in Low was significantly enhanced, but the positive expression level of LC3 in High was not significantly higher than that in Con.

Summary statistics of 16S rRNA raw sequencing data

The cecum contents were subjected to 16S rRNA sequencing, and the 16S rRNA raw data was obtained by high-throughput sequencing on the Illumina platform. First, after quality control of the original sequence, a total of 1,558,718 clean tags were obtained. After chimera filtering, 1,167,744 effective tags that could be used for subsequent analysis were finally obtained. According to the data of effective tags, the OTUs were clustered with 97 % similarity. A total of 4886 OTUs were obtained, with an average of 271 OTUs obtained for each sample. The shared and unique OTUs between the three different groups were analyzed and the Venn diagram were plotted. The result is shown in Fig. 4(a). We find that there are 1123 OTU shared by the three groups, the unique OTU number of Con is 601, the unique OTU number of Low is 270, and the unique OTU number of High is 609, indicating that the number of OTUs available in Low is the least.

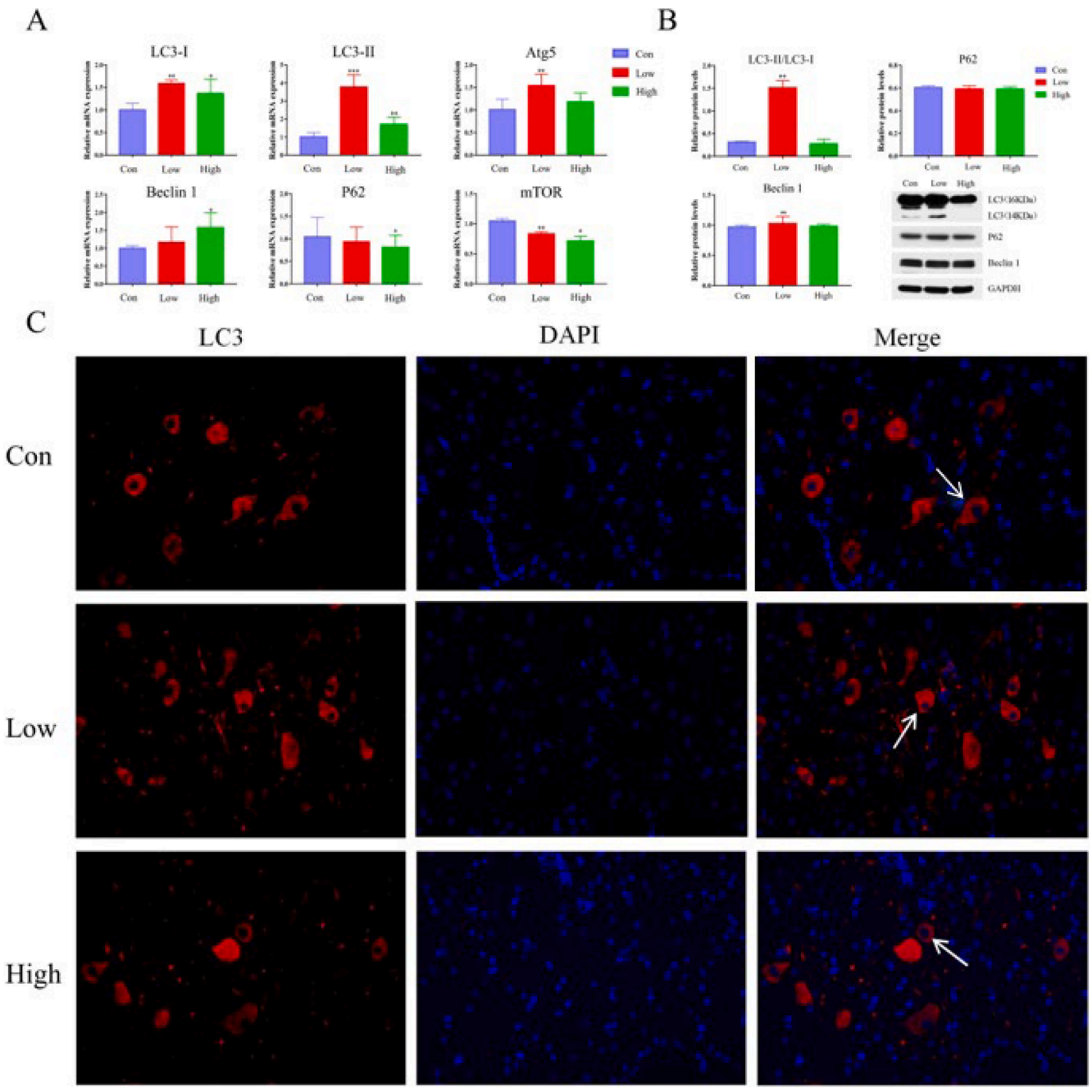

Fig. 3. Effects of dichlorvos on cerebellar autophagy in broilers.
A: Effects of dichlorvos on mRNA expression of autophagy-related genes in cerebellum. B: Effects of dichlorvos on the expression levels of autophagy-related proteins in cerebellum. C: Immunofluorescent analysis of LC3 in cerebellum (400 ×). Cells stained in red are LC3 positive (white arrow).(*:$P<0.05$,**:$P<0.01$,***:$P<0.001$)

Alpha and beta diversity of the microbiota

Rarefaction curves are shown in Fig. 4(b). With the increase in sequencing number, the curves of each group tend to be flat gradually, and the identification of new OTUs was less and less, indicating that the current sequencing depth was sufficient to cover the diversity of all microorganisms in each sample. When the sequencing depth was between 50,000 and 60,000, the number of OTUs in each group showed the pattern that Con>High>Low at the same sequencing depth. This also indicated that the diversity of bacteria in Low and High was lower than that in Con.

The alpha index of different samples was based on the 97 % consistency threshold. The difference between the groups was analyzed for the alpha diversity index, and the significance of the difference in species diversity between the groups was analyzed by Wilcoxon rank sum test and Tukey's test and a box plot was drawn. The results are shown in Fig. 4(c). Compared with Con, Low significantly reduced Chao1 and ACE ($P<0.05$), and significantly increased Simpson ($P<0.05$), indicating that the richness and diversity of broilers in Low decreased. In addition, High significantly improved Simpson ($P<0.05$), while Chao1 and ACE showed a rising trend, but the difference was not statistically significant ($P>0.05$), indicating that the evenness and richness of the broilers in High were similar to the control group. Similarly, this corresponds exactly to the result of the rarefaction curves.

The results of principal coordinate analysis (PCoA) are shown in Fig. 4(d). Only one sample in Con has a large degree of dispersion, and

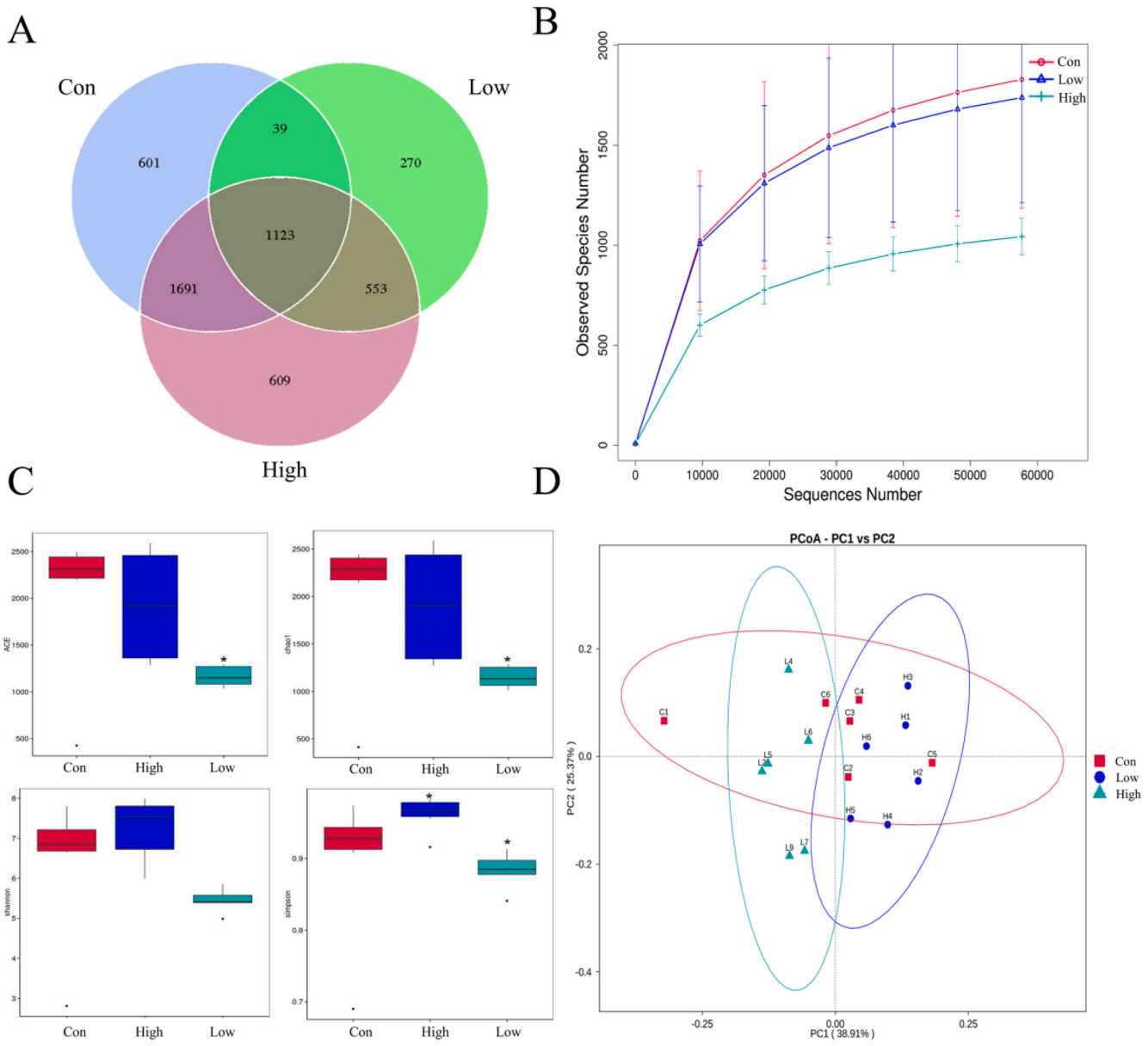

Fig. 4. Alpha diversity and Beta diversityof the microbiota (n=6).
A: Representation of the OTUs between different groups via a Venn diagram. B: Rarefaction curves. C: Comparison of alpha diversity indices. D: Principal coordinate analysis plots (PCoA).(*:$P<0.05$)

the distances between the other five samples is relatively small. The distance between the samples of Low and High is small, and there is no obvious separation, indicating that the microbial community structure of each group is similar, and there is not much difference. In addition, the caecal flora of broiler chickens has no obvious distance between Low, High, and Con. Instead, there is a shared region, which indicates that the microbial flora of the cecal microbial broilers of the three experimental groups have a certain similarity. Although there is overlap, each group has parts independent of the other two groups, which proves that the microbiota of the three groups has both similarities and differences.

Analysis of the level of difference between groups

In order to find the different species between the groups at the phylum and genus level, we did a T-test between groups. The relative abundance results at the phylum level are shown in Fig. 5(a). At the phylum level, the relative abundance of *Cyanobacteria* in Low increased significantly ($P<0.01$). The relative abundances of *Methylomirabilota, Nitrospirota, Armatimonadota, Fusobacteriota, Myxococcota, Planctomycetota, Acidobacteriota, Chloroflexi* and *unidentified bacteria* were significantly reduced ($P<0.05$ or $P<0.01$). In High, only the relative abundance of *Fusobacteriota* decreased significantly ($P<0.05$), and there were no phyla with relative abundance increased. This shows that the destruction of intestinal flora in Low is more serious than that in High.

The relative abundance at the genus level is shown in Fig. 5(b). Compared with Con, the relative abundance of *unidentified Chloroplast, unidentified Mitochondria, Escherichia Shigella, Enterococcus* and *Allorhizobium-Neorhizobium-Pararhizobium-Rhizopbium* in Low increased significantly ($P<0.05$ or $P<0.01$); The relative abundance of *Neisseria, Porphyromonas, Prevotella, Actinomyces, Capnocytophaga, Gaiella, Candidatus Kuenenia, Limnobacter, Cardiobacterium, unidentified SJA-28, Tannerella, Arthrobacter, Bryobacter, Acidibacter, Solirubrobacter, Bradyrhizobium, OLB13, Nocardioides* and *Thermomonas* decreased

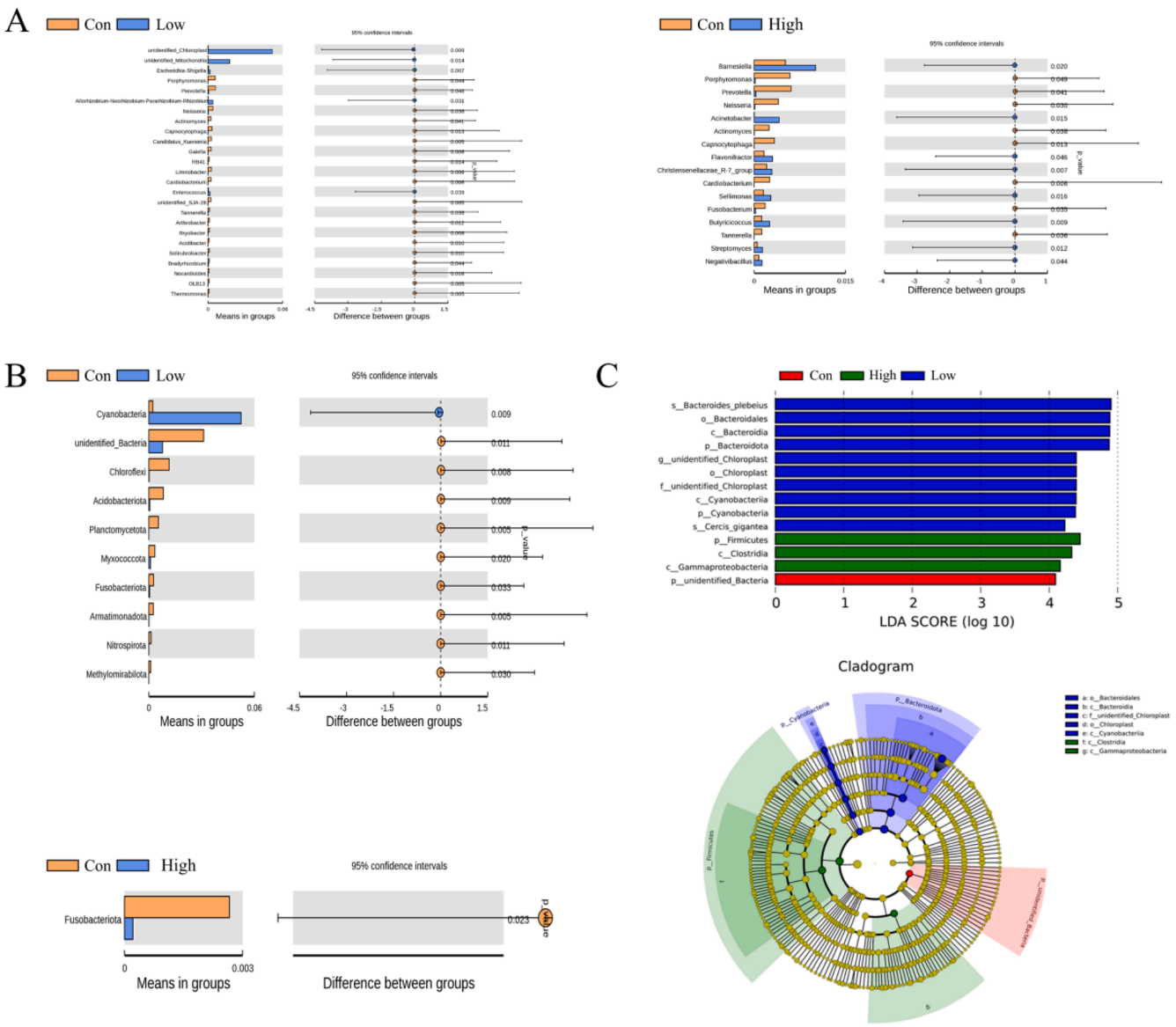

Fig. 5. Analysis of species differences between groups.
A: The difference in species analysis between group according to a T-test at phylum level. B: The difference in species analysis between group according to a T-test at genus level. C: LEFse analysis on caecum microbiota.

significantly ($P<0.05$ or $P<0.01$). The relative abundance of *Barnesiella, Acinetobacter, Flavonifractor, Christensenellaceae R-7 group, Cardiobacterium, Sellimonas, Butyricicoccus* and *Negativibacillus* in High increased significantly ($P<0.05$ or $P<0.01$). The relative abundance of *Porphyromonas, Prevotella, Neisseria, Actinomyces, Capnocytophaga, Fusobacterium* and *Tannerella* decreased significantly ($P<0.05$ or $P<0.01$).

LefSe analysis

LEfSe (Linear discriminant analysis effect size) analysis was used to find species with significant differences between different groups. The analysis method was mainly based on evaluating the LDA effect size, combining LDA with the non-parametric Kruskal-Walli's test and Wilcoxon rank sum test to screen out the different communities between different groups. When the LDA score is higher than 2, it means that the relative abundance of the corresponding group is significantly higher than that of the other two groups, that is, $P<0.05$. The results of LEfSe analysis are shown in Fig. 5(c). We found *Bacteroidota, Chloroplast, Cyanobacteria* and *Cercis gigantea* in Low were significantly higher than the other two groups (LDA>2). *Firmicutes, Clostridia* and *Gammaproteobacteria* in High were significantly higher than the other two groups (LDA>2). The unidentified bacteria in Con were significantly higher than the other two groups (LDA>2).

Functional prediction of intestinal microbial community

In order to explore the effect of acute dichlorvos exposure on the metabolic function of cecal flora in broilers, the functional changes of 16S rRNA genes in cecal microflora after dichlorvos exposure were predicted by comparing the biological metabolic functions of PICRUSt and KEGG database. Top 35 functions in terms of abundance were selected, and a heatmap was made to show their abundance information. As shown in Fig. 6(a), the intestinal flora in Low showed a significant positive correlation with the relative abundance of *Genetic Information Processing* and *Human Diseases genes*, and a significant negative correlation with the relative abundance of *Cellular Processes* genes. The intestinal flora in the high - dose group showed a significant positive

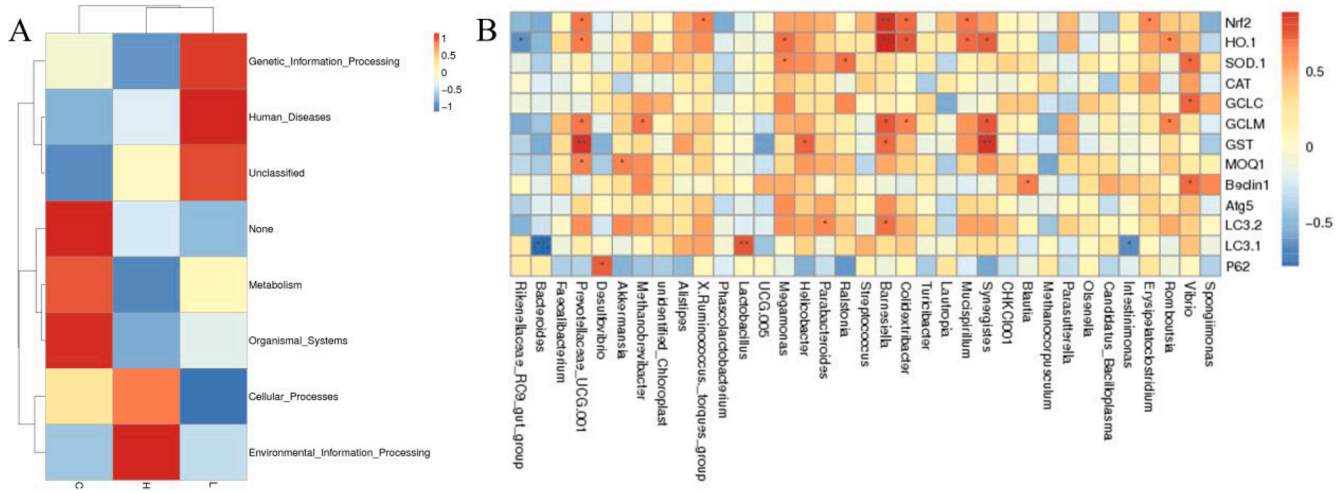

Fig. 6. Thermography analysis.
A: Microbiome function prediction according to KEGG-L1 pathway database. B: Relationships between autophagy-related genes and the compositions of microbiota.

correlation with the relative abundance of the *Environmental Information Processing* gene and a significant negative correlation with the relative abundance of the *Genetic Information Processing* gene. There was a significant positive correlation between the intestinal flora and the relative abundance of *Organismal Systems* gene in Con.

Correlation analysis

Fig. 6(b) shows the relationship between the relative abundance of cecal flora composition and the expression of antioxidant-related genes and autophagy-related genes. Spearman rank correlation was used to analyze the relationship between gene table and microbial species richness (alpha diversity) at the phylum level, so as to obtain the correlation and significance P value between the two. The results showed that the relative abundance of the Nrf2 gene was significantly positively correlated with the relative abundance of 19 phyla including *Crenarchaeota, Latescibacterota, NB1.j, Gemmatimonadetes, Deinococcota, RCP2.54, Gemmatimonadota, Planctomycetes, Methylomirabilota, Nitrospirota, Armatimonadota, Myxococcota, Planctomycetota, Deferribacteres, Acidobacteriota, Chloroflexi, Verrucomicrobiota, Proteobacteria* and *Firmicutes* ($P<0.05$ or $P<0.01$), whereas it was significantly negatively correlated with the relative abundance of *Bacteroidota* ($P<0.01$). The relative abundance of the HO-1 gene was significantly positively correlated with *Bdellovibrionota, Nitrospirota, Armatimonadota, Planctomycetota, Synergistota, Deferribacteres, Acidobacteriota, Verrucomicrobiota* and *Firmicutes* ($P<0.05$ or $P<0.01$), whereas it was significantly negatively correlated with the relative abundance of *Bacteroidota* ($P<0.01$). The relative abundance of genes GST and GCLC was significantly negatively correlated with the relative abundance of *Fusobacteriota* ($P<0.01$). The relative abundance of the GCLM gene was significantly positively correlated with the relative abundance of *Synergistota, Euryarchaeota, Verrucomicrobiota* and *Firmicutes* ($P<0.05$ or $P<0.01$), whereas it was significantly negatively correlated with the relative abundance of *Bacteroidota* ($P<0.05$). The relative abundance of the GST gene was significantly positively correlated with the relative abundance of *Armatimonadota, Planctomycetota, Synergistota, Acidobacteriota, Verrucomicrobiota* and *Firmicutes* ($P<0.05$ or $P<0.01$), whereas it was significantly negatively correlated with the relative abundance of *Bacteroidota* ($P<0.05$). The relative abundance of the Beclin1 gene was significantly negatively correlated with the relative abundance of *Spirochaetota* and *Fusobacteriota* ($P<0.05$). The relative abundance of the Atg5 gene was significantly negatively correlated with the relative abundance of *Fusobacteriota* ($P<0.01$). The relative abundance of gene LC3 was significantly positively correlated with *Firmicutes* ($P<0.01$), whereas it was significantly negatively correlated with the relative abundance of Fusobacteriota and Bacteroidota ($P<0.05$ or $P<0.01$). The relative abundance of the P62 gene was significantly positively correlated with the relative abundance of *Desulfobacterota* ($P<0.05$), whereas it was significantly negatively correlated with the relative abundance of *Cyanobacteria* ($P<0.01$).

Discussion

There has been evidence of neurotoxicity, hepatotoxicity, nephrotoxicity, immunotoxicity, reproductive toxicity and carcinogenicity of dichlorvos (Mennear, 1994; Salahshoor et al., 2020). However, there are limited studies on the toxic effects of dichlorvos on other tissues. In this study, obvious pathological changes were found in the cerebellum and cecum of dichlorvos-exposed broilers. Recent studies have shown that there is a correlation between brain and gut pathomechanisms in the development of diseases (Carloni and Rescigno, 2023; Xie et al., 2022). In order to expore brain and gut interrelation in the toxicological process of dichlorvos in broiler chickens.,test the expression levels of relevant genes, which it was found that significant oxidative stress and cellular autophagy occurred in the cerebellum of broilers in the low-dose dichlorvos-exposed group (Abadeen, 2021). In order to explore the possible pathogenesis, we analysed the changes in cecum flora by metabolomics technology and did correlation analysis between the two and found that the relative abundance of autophagy-related genes such as Nrf2 was significantly correlated with some specific bacteria. This is the first study to examine how intestinal microbiota function changed in response to acute dichlorvos exposure in broilers, and to analyze the relationship between cerebellum autophagy and intestinal microbiota after dichlorvos exposure.

According to our previous studies, acute dichlorvos exposure has the most obvious damage to the cerebellum of broilers (Huang et al., 2022). Many studies have shown that no matter what form of dichlorvos exposure, it can be transported to the brain area through the blood-brain barrier, causing neuronal damage and neurotoxicity (Michinaga and Koyama, 2015). In our research, we found that after exposure to dichlorvos, the cerebellar sulci of the cerebellum became larger, the glial cells appeared to show morphological changes, Purkinje cells deformed or formed vacuoles, and the granular cells also showed obvious shrinkage and deformation. It shows that acute dichlorvos exposure destroys the normal morphology of the cerebellum and causes damage to the cerebellum.

There is evidence that dichlorvos exposure can destroy the balance of ROS/antioxidant system, lead to the production and accumulation of

reactive oxygen species (ROS), and cause oxidative damage (Rambabu et al., 2020). In this study, dichlorvos exposure enhanced the content of SOD, T-AOC, MDA and the expression of Nrf2, HO-1, SOD-1, CAT, GSH, GCLC, GCLM and NQO1 mRNA in cerebellum. However, no significant difference between CAT and Con was found in the determination of enzyme activity or mRNA expression. Superoxide dismutase (SOD) and catalase (CAT) are the first line of defense in the antioxidant system. They initiate the body's protective mechanism against oxidative stress. As a key enzyme for scavenging oxygen free radicals, SOD plays a key role in catalyzing the disproportionation of superoxide free radicals to hydrogen peroxide (Coimbra-Costa et al., 2017). CAT is an enzyme located in the peroxisome of cells. Its main function is to remove excess hydrogen peroxide in the body. Therefore, SOD and CAT can be considered as important indicators to measure antioxidant capacity or reactive oxygen species-mediated oxidative damage. In addition, antioxidant capacity can be indirectly determined by estimating the activity of total antioxidant capacity (T-AOC) or the content of lipid peroxidation products represented by malondialdehyde (MDA) (Hundekari et al., 2013). As the main transcription factor in the antioxidant defense system, Nrf2 has an adaptive protective effect on oxidative stress in cells. It will up-regulate a variety of downstream target genes responsible for cell protection, such as HO-1, GCLC, GCLM, NQO1 and GST. HO-1 is an important enzyme with significant antioxidant activity and protective effect against antioxidant damage. GCLC and GCLM constitute two important subunits of GCL rate limiting enzyme, which is a key factor in maintaining intracellular glutathione (GSH) homeostasis (Xu et al., 2016). NQO1 can catalyze the two-electron reduction of quinone compounds, remove excess superoxide in the body, and protect tissues or cells from oxidative damage. GST is a phase II biotransferase that helps to couple electrophilic toxic molecules to GSH, which is also considered to be an important part of the antioxidant defense mechanism (Ni et al., 2019). As one of the key enzymes of the antioxidant (Zhao et al., 2021) defense system in the organism, it has been pointed out that the activity of CAT can have an inhibition period, its activity can be inhibited in the excitation period, and its activity will recover in the recovery period. Our results show that after acute poisoning in broilers, it may be that the production of cerebellar ROS exceeds the threshold, which inhibits the activity of CAT. When the level of ROS starts to decrease and is back within the threshold, the activity of CAT may gradually increase. The above studies show that acute dichlorvos exposure can induce oxidative stress in the cerebellum of broilers, and enhance antioxidant capacity by activating the Nrf2 pathway in the cerebellum to protect cerebellar cells from oxidative damage.

Under certain pathological conditions, such as toxic injury, intracellular homeostasis is disrupted by the excessive accumulation of reactive oxygen species, leading not only to oxidative stress in tissues but also to cell autophagy (Yang et al., 2018). Therefore, in this study, we also investigated the effect of autophagy on toxic damage to cerebellum caused by dichlorvos. In the process of autophagy, misfolded proteins and damaged organelles are enveloped by a bilayer membrane structure to form autophagosomes, which are then transported to lysosomes for degradation, involving a number of autophagy-related proteins. Beclin1 and LC3 are two important markers of autophagy that are closely associated with the process of autophagy, especially in the early stages. Beclin1 is a key protein that serves as a cofactor in the formation of the Beclin1-Vps34-Vps15 complex. Its main function is to trigger a series of proteins involved in autophagic lysosome formation (Li et al., 2015). LC3 is referred to as a lysosome-related protein and is therefore commonly used to determine the degree of autophagy. There are two main forms of LC3: LC3-I and LC3- II. It has been confirmed that LC3- II is a combination of LC3-I and phosphatidylethanolamine, and its main function is to participate in the formation of the membrane of the autophagy body. Therefore, the ratio of LC3- II to LC3-I, i.e. LC3- II / LC3-I, is directly proportional to the number of autophagosomes, and is also a general recognition index that can directly reflect the degree of autophagy (Xu et al., 2016). In addition, Atg5 is also involved in regulating autophagosome membrane formation, which is also required for LC3 lipidation and targeting (Zhao et al., 2021). P62, an autophagy marker, is also the first protein reported to have an adaptor function in autophagy that is degraded by autophagy activation (Bjorkoy et al., 2006).

In addition, mTOR has been confirmed to be closely associated with the regulation of autophagy and cellular metabolism (Saxton and Sabatini, 2017). Yang et al. found that dichlorvos can induce autophagy in Sk-N- SH cells and mRNA expression of autophagy-related genes also increased (Yang et al., 2019). Compared with the Con, the mRNA expressions of Beclin1, Atg5, LC3-I and LC3- II were upregulated to some extent, while the mRNA expression of P62 was downregulated. Compared with the Con, the expression of Beclin1 and LC3- II / LC3-I protein significantly increased in the treatment group, while the expression of P62 protein significantly decreased. Moreover, immunoblotting and immunofluorescence analysis showed that exposure to low-dose dichlorvos increased the positive expression of Beclin1 and LC3- II in the cytoplasm of cerebellum, but there was no significant change in the high-dose group, because our experiment was designed as an acute poisoning experiment and the experimental broilers in the High would die within 15 minutes and the sampling would be completed. It has been suggested in the literature that protein expression lags behind mRNA expression up to 3 hours (Zhao et al., 2021), which also shows that the cerebellum of the high dose broilers has started the transcription process of autophagy related genes while the translation process has not yet started. These results suggest that acute dichlorvos exposure can induce cerebellar autophagy, implying that when acute dichlorvos exposure results in cerebellar injury, the cerebellar autophagy level is improved to some extent, which may indicate that under the condition of dichlorvos poisoning, the occurrence of autophagy protects the cells from the oxidative damage of the cerebellum caused by dichlorvos poisoning to maintain the homeostasis of cerebellar cells.

Our results showed that exposure to dichlorvos significantly increased the thickness of cecal muscle layer, which might be related to intestinal spasm..Studies have shown that acute dichlorvos exposure can also lead to increased accumulation in the intestine, stimulate sympathetic ganglia, release norepinephrine, cause vasospasm of the intestinal wall, disruption of microcirculation, secondary infection, and ischemia and necrosis of the intestinal wall due to sepsis. This also shows that acute dichlorvos poisoning damages the intestine (Changsheng et al., 2019). In addition, our experimental results showed that exposure to dichlorvos resulted in shortening or rupture of cecal villi, atrophy of intestinal glands, and reduction in the number of goblet cells, suggesting that dichlorvos may cause intestinal injury in broiler chickens. Our results also showed that acute dichlorvos exposure affected the diversity of microbiota in the appendix of broiler chickens. Further analysis showed that compared with the control group, Chao1 index and ACE index decreased and Simpson index increased in the two exposure groups. These results suggest that acute dichlorvos exposure significantly alters microbial diversity.16S rRNA sequencing of microorganisms in the caecum of broiler chickens showed that dichlorvos exposure reduced the relative abundance of Methylomirabilota, Nitrospirota, Armatimonadota, Fusobacteriota, Myxococcota, Planctomycetota, Acidobacteriota, and Chloroflexi. Previous reports have also highlighted that the gut microbiota may play a key role in limiting the uptake of toxins in the gut (Zhou et al., 2018). However, if the balance of these gates is disrupted, it may expand the intestinal absorption of these toxins and further exacerbate toxicity (Breton et al., 2013). Therefore, exposure to dichlorvos will destroy the balance of microorganisms in the gut and make the intestinal tract more susceptible to infection. At the genus level, the relative abundance of 29 species such as Actinomyces, Acidibacter, Acinetobacter, and Actinomyces significantly decreased in the cecum of the dichlorvos-treated group, while the relative abundance of 14 species such as Escherichia Shigella, Barnesiella, and Streptomyces significantly increased. Infection of chickens with Streptomyces, also known as avian cholera, is characterized by fever, diarrhea, and respiratory distress, and

most acute cases die quickly (Botzler, 2002). This also explains that acute exposure to dichlorvos seriously destroys the diversity of the microbial community in broiler chickens, increases the relative abundance of harmful bacteria, destroys the stable state of the gut microbiota, and increases the incidence of some diseases in broiler chickens.The role of the animal intestinal microbiome in human and animal metabolism is evidence of this. By comparative analysis of 16S rRNA gene sequencing results, we evaluated the effect of acute dichlorvos exposure on the predictive function of the cecal microflora in broilers. Our results showed that there was a significant positive correlation between intestinal flora and genetic information processing gene, human disease gene, and environmental information processing gene after dichlorvos exposure. When we see the word "genetic information", we first think of the central law. Our prediction results show that acute dichlorvos exposure can affect genetic molecular processes such as DNA replication, DNA transcription and RNA translation. Human disease genes include those related to cancer and metabolic diseases. Environmental information may mean that some bacteria in the gut have a specific relationship with the environment. Based on these bacteria, the level of environmental pollution can be evaluated in the future. Our prediction results show that acute dichlorvos exposure can increase the risk of metabolic diseases and cancer, destroy the normal molecular regulatory mechanism of the body, and damage the environment.

According to our results, there are no less than 20 bacteria associated with Nrf2 gene. It turns out that the microorganisms of the intestine are closely related to the antioxidant capacity of the body. Lactobacillus is a widely used beneficial bacteria in the body, including Bifidobacterium and Lactobacillus, which are probiotics in the list of probiotic strains of natural foods. It turns out that these probiotics are closely related to the antioxidant capacity of the body (Khan, 2019).The common proteus bacteria are pathogenic bacteria such as Escherichia, Salmonella and Helicobacter. These pathogenic bacteria can cause gastrointestinal infections or damage to multiple organs and are very infectious (Hafez, 2011). According to our results, these pathogenic bacteria also have some relationship with the antioxidant capacity of the body. In addition, our results showed that the expression of LC3 gene was significantly positively correlated with the relative abundance of Firmicutes. There was a significant negative correlation with the relative abundance of Fusobacteriota and Bacteroidota (Wang, 2019). As we all know, Firmicutes and Bacteroidetes in the gut are two important bacteria that influence the degree of obesity and thinness. Research shows that obese people have about 20Carloni and Rescigno, 2023 % more Firmicutes than slim people and about 90 % less Bacteroides than slim people (Yuan et al., 2018). According to our analysis results, we speculate that Firmicutes and Bacteroidetes are related not only to obesity but also to the expression of LC3 gene, but the specific relationship needs further research. Clostridium is mainly distributed in the oral cavity, upper gastrointestinal tract, intestinal tract, and urogenital tract of animals, especially in oral tartar, but it also has some pathogenicity that can cause pseudomembranous enteritis (Park et al., 2008). Our results indicate that Clostridium pathogenicity may be related to the expression of the autophagy-related gene LC3, which also provides a new research basis for future research on Clostridium. The results of our correlation analysis show that the mRNA expression of genes related to autophagy and oxidative stress is related to some specific bacteria, which may also provide a new research direction for the study of the mechanism of autophagy and oxidative stress or the mechanism of bacteria on the body in the future.

Conclusion

Acute exposure to dichlorvos destroyed the normal histological morphology of cerebellar neurons, induced oxidative stress and autophagy in the cerebellum, and damaged the cerebellum of broilers. Furthermore, acute dichlorvos exposure destroys the normal histological morphology of broiler chicken appendix, causes damage to the appendix, alters the microbial composition, structure, and flora diversity of broiler chicken appendix, reduces the microbial richness and diversity of the appendix, and alters its metabolic spectrum. In addition, up- or down-regulation of mRNA expression of autophagy-related genes is related to some specific bacteria.

Ethics approval and consent to participate

The authors declare that this article is reported in accordance with the ARRIVE guidelines. All experiments were conducted in accordance with relevant guidelines and regulations, and all protocols were approved by the Committee for the Care and Use of Laboratory Animals of Jiangxi Agricultural University, China (No. JXAULL-202045).

Funding

This project was supported by the National Natural Science Foundation of China Youth Science Fund Project (No. 32460906),the Jiangxi Provincial Natural Science Foundation General Project (No. 20224BAB205033).

CRediT authorship contribution statement

Juan Chen: Formal analysis, Writing – original draft, Writing – review & editing, Validation. **Yun Zhang:** Methodology, Writing – review & editing. **Chenxi Jiang:** Formal analysis, Writing – original draft. **Shupeng Chen:** Data curation, Validation, Formal analysis. **Yulan Zhao:** Writing – original draft, Data curation, Validation, Formal analysis. **Xiaona Gao:** Methodology, Formal analysis. **Xiaoquan Guo:** Methodology, Visualization, Resources, Funding acquisition. **Guoliang Hu:** Validation, Resources, Funding acquisition. **Pei Liu:** Methodology, Formal analysis. **Huibo Jin:** Writing – original draft, Data curation, Validation, Formal analysis. **Ying Zhang:** Data curation, Validation, Formal analysis. **Salma Mbarouk Omar:** Validation, Formal analysis. **Lin Li:** Data curation, Validation. **Gen Wan:** Formal analysis, Writing – review & editing. **Ping Liu:** Software, Conceptualization, Writing – review & editing, Supervision, Project administration, Funding acquisition.

Declaration of competing interest

The authors declare that they have no known competing financial interests or personal relationships that could have appeared to influence the work reported in this paper.

Acknowledgements

Thanks to all the people who helped in the experiment and writing, and to the teachers for their money and scientific research help.

References

Abadeen, Z.U., 2021. alutary effects of anti-Clostridium perfringens type A egg yolk antibodies (IgY) on growth performance and hemato-biochemical parameters in experimentally infected broiler chicken. Pak. Vet. J. 41 (04), 562–566.

Akami, M., Njintang, N.Y., Gbaye, O.A., Andongma, A.A., Rashid, M.A., Niu, C.Y., Nukenine, E.N., 2019. Gut bacteria of the cowpea beetle mediate its resistance to dichlorvos and susceptibility to Lippia adoensis essential oil. Sci. Rep. 9 (1), 6435.

Al-Zubaidy, M.H., Mousa, Y.J., Hasan, M.M., Mohammad, F.K., 2011. Acute toxicity of veterinary and agricultural formulations of organophosphates dichlorvos and diazinon in chicks. Arh. Hig. Rada Toksikol. 62 (4), 317–323.

Antonijevic, E., Kotur-Stevuljevic, J., Musilek, K., Kosvancova, A., Kuca, K., Djukic-Cosic, D., Spasojevic-Kalimanovska, V., Antonijevic, B., 2018. Effect of six oximes on acutely anticholinesterase inhibitor-induced oxidative stress in rat plasma and brain. Arch. Toxicol. 92 (2), 745–757.

Ben, S.I., Boussabbeh, M., Pires, D.S.J., Saidi, N.E., Abid-Essefi, S., Lemaire, C., 2023. Effects of Dichlorvos on cardiac cells: toxicity and molecular mechanism of action. Chemosphere 330, 138714.

Bjorkoy, G., Lamark, T., Johansen, T., 2006. p62/SQSTM1: a missing link between protein aggregates and the autophagy machinery. Autophagy. 2 (2), 138–139.

Borodkina, A.V., Shatrova, A.N., Deryabin, P.I., Grukova, A.A., Nikolsky, N.N., Burova, E. B., 2016. Tetraploidization or autophagy: the ultimate fate of senescent human endometrial stem cells under ATM or p53 inhibition. Cell Cycle 15 (1), 117–127.
Botzler, R.G., 2002. Avian cholera on north coast California: distinctive epizootiological features. Ann. N. Y. Acad. Sci. 969, 224–228.
Breton, J., Daniel, C., Dewulf, J., Pothion, S., Froux, N., Sauty, M., Thomas, P., Pot, B., Foligne, B., 2013. Gut microbiota limits heavy metals burden caused by chronic oral exposure. Toxicol. Lett. 222 (2), 132–138.
Bui-Nguyen, T.M., Baer, C.E., Lewis, J.A., Yang, D., Lein, P.J., Jackson, D.A., 2015. Dichlorvos exposure results in large scale disruption of energy metabolism in the liver of the zebrafish, Danio rerio. BMC. Genomics. 16, 853.
Carloni, S., Rescigno, M., 2023. The gut-brain vascular axis in neuroinflammation. Semin. Immunol. 69, 101802.
Changsheng, L., Heliu, D., Zhicheng, F., Xianyi, Y., Lin, C., Hui, G., 2019. Portal vein gas and pneumatosis intestinalis: A case of intestinal necrosis caused by acute organophosphorus pesticide poisoning? Toxicol. Ind. Health 35 (7), 482–485.
Chen, L.J., Zhi, X., Zhang, K.K., Wang, L.B., Li, J.H., Liu, J.L., Xu, L.L., Yoshida, J.S., Xie, X.L., Wang, Q., 2021. Escalating dose-multiple binge methamphetamine treatment elicits neurotoxicity, altering gut microbiota and fecal metabolites in mice. Food Chem. Toxicol. 148, 111946.
Coggon, D., 2002. Work with pesticides and organophosphate sheep dips. Occup. Med. (Lond) 52 (8), 467–470.
Coimbra-Costa, D., Alva, N., Duran, M., Carbonell, T., Rama, R., 2017. Oxidative stress and apoptosis after acute respiratory hypoxia and reoxygenation in rat brain. Redox. Biol. 12, 216–225.
Dwivedi, N., Flora, G., Kushwaha, P., Flora, S.J., 2014. Alpha-lipoic acid protects oxidative stress, changes in cholinergic system and tissue histopathology during co-exposure to arsenic-dichlorvos in rats. Environ. Toxicol. Pharmacol. 37 (1), 7–23.
Hafez, H.M.F.U, 2011. Enteric diseases of poultry with special attention to Clostridium perfringens. Pak Vet J 31 (3), 175–184.
Huang, L., Guo, X., Liu, P., Zhao, Y., Wu, C., Zhou, C., Huang, C., Li, G., Zhuang, Y., Cheng, S., Cao, H., Zhang, C., Xu, Z., Liu, X., Hu, G., Liu, P., 2022. Correlation between acute brain injury and brain metabonomics in dichlorvos-poisoned broilers. J. Hazard. Mater. 422, 126849.
Hundekari, I.A., Suryakar, A.N., Rathi, D.B., 2013. Acute organo-phosphorus pesticide poisoning in North Karnataka, India: oxidative damage, haemoglobin level and total leukocyte. Afr. Health Sci. 13 (1), 129–136.
Khan, M., 2019. Effect of newly characterized probiotic lactobacilli on weight gain, immunomodulation and gut microbiota of Campylobacter jejuni challenged broiler chicken. Pak. Vet. J. 39 (0253-8318), 473–478.
Kwong, T.C., 2002. Organophosphate pesticides: biochemistry and clinical toxicology. Ther. Drug Monit. 24 (1), 144–149.
Li, D., Yao, H., Li, Y., Li, Z., Yang, X., Zhu, X., Zeng, X., 2023. Thallium(III) exposure alters diversity and co-occurrence networks of bacterial and fungal communities and intestinal immune response along the digestive tract in mice. Environ. Sci. Pollut. Res. Int. 30 (13), 38512–38524.
Li, J.P., Yang, Y.X., Liu, Q.L., Zhou, Z.W., Pan, S.T., He, Z.X., Zhang, X., Yang, T., Pan, S. Y., Duan, W., He, S.M., Chen, X.W., Qiu, J.X., Zhou, S.F., 2015. The pan-inhibitor of Aurora kinases danusertib induces apoptosis and autophagy and suppresses epithelial-to-mesenchymal transition in human breast cancer cells. Drug Des. Devel. Ther. 9, 1027–1062.
Li, W., Deng, Y., Chu, Q., Zhang, P., 2019. Gut microbiome and cancer immunotherapy. Cancer Lett. 447, 41–47.
Mennear, J.H., 1994. Dichlorvos carcinogenicity: an assessment of the weight of experimental evidence. Regul. Toxicol. Pharmacol. 20 (3 Pt 1), 354–361.
Michinaga, S., Koyama, Y., 2015. Pathogenesis of brain edema and investigation into anti-edema drugs. Int. J. Mol. Sci. 16 (5), 9949–9975.
Mohammad, F.K., Al-Badrany, Y.M., Al-Jobory, M.M., 2008. Acute toxicity and cholinesterase inhibition in chicks dosed orally with organophosphate insecticides. Arh. Hig. Rada Toksikol. 59 (3), 145–151.
Ni, H., Peng, L., Gao, X., Ji, H., Ma, J., Li, Y., Jiang, S., 2019. Effects of maduramicin on adult zebrafish (Danio rerio): acute toxicity, tissue damage and oxidative stress. Ecotoxicol. Environ. Saf. 168, 249–259.
Park, S.S., Lillehoj, H.S., Allen, P.C., Park, D.W., FitzCoy, S., Bautista, D.A., Lillehoje, E. P., 2008. Immunopathology and cytokine responses in broiler chickens coinfected with Eimeria maxima and Clostridium perfringens with the use of an animal model of necrotic enteritis. Avian Dis. 52 (1), 14–22.
Rambabu, L., Megson, I.L., Eddleston, M., 2020. Does oxidative stress contribute to toxicity in acute organophosphorus poisoning? - a systematic review of the evidence. Clin. Toxicol. (Phila) 58 (6), 437–452.
Ruan, Y., Wu, C., Guo, X., Xu, Z., Xing, C., Cao, H., Zhang, C., Hu, G., Liu, P., 2019. High doses of copper and mercury changed cecal microbiota in female mice. Biol. Trace Elem. Res. 189 (1), 134–144.
Rusyniak, D.E., Nanagas, K.A., 2004. Organophosphate poisoning. Semin. Neurol. 24 (2), 197–204.
Salahshoor, M.R., Abdolmaleki, A., Shabanizadeh, A., Jalali, A., Roshankhah, S., 2020. Ipomoea aquatica extract reduces hepatotoxicity by antioxidative properties following dichlorvos administration in rats. Chin. J. Physiol. 63 (2), 77–84.
Saxton, R.A., Sabatini, D.M., 2017. mTOR signaling in growth, metabolism, and disease. Cell 168 (6), 960–976.
Wang, J., 2019. Protective effects of Baicalein against cadmium-induced oxidative stress in rat testes. Pak. Vet. J. 39 (0253-8318), 216–220.
Wu, K., Liu, M., Wang, H., Rajput, S.A., Al, Z.O., Wang, S., Qi, D., 2023. Effect of zearalenone on aflatoxin B1-induced intestinal and ovarian toxicity in pregnant and lactating rats. Ecotoxicol. Environ. Saf. 258, 114976.
Xie, Z., Zhang, X., Zhao, M., Huo, L., Huang, M., Li, D., Zhang, S., Cheng, X., Gu, H., Zhang, C., Zhan, C., Wang, F., Shang, C., Cao, P., 2022. The gut-to-brain axis for toxin-induced defensive responses. Cell 185 (23), 4298–4316.
Xu, X.R., Yu, H.T., Yang, Y., Hang, L., Yang, X.W., Ding, S.H., 2016. Quercetin phospholipid complex significantly protects against oxidative injury in ARPE-19 cells associated with activation of Nrf2 pathway. Eur. J. Pharmacol. 770, 1–8.
Yang, F., Liao, J., Pei, R., Yu, W., Han, Q., Li, Y., Guo, J., Hu, L., Pan, J., Tang, Z., 2018. Autophagy attenuates copper-induced mitochondrial dysfunction by regulating oxidative stress in chicken hepatocytes. Chemosphere 204, 36–43.
Yang, Y., Wen, C., Zheng, S., Liu, W., Chen, J., Feng, X., Wang, X., Yang, F., Ding, Z., 2019. Influence of microcystins-LR (MC-LR) on autophagy in human neuroblastoma SK-N-SH cells. J. Toxicol. Environ. Health a 82 (21), 1129–1136.
Yuan, M., Li, D., Zhang, Z., Sun, H., An, M., Wang, G., 2018. Endometriosis induces gut microbiota alterations in mice. Hum. Reprod. 33 (4), 607–616.
Zhang, X.Y., Chen, J., Yi, K., Peng, L., Xie, J., Gou, X., Peng, T., Tang, L., 2020. Phlorizin ameliorates obesity-associated endotoxemia and insulin resistance in high-fat diet-fed mice by targeting the gut microbiota and intestinal barrier integrity. Gut. Microbes. 12 (1), 1–18.
Zhao, Y., Zhou, C., Wu, C., Guo, X., Hu, G., Wu, Q., Xu, Z., Li, G., Cao, H., Li, L., Latigo, V., Liu, P., Cheng, S., Liu, P., 2020. Subchronic oral mercury caused intestinal injury and changed gut microbiota in mice. Sci. Total. Environ. 721, 137639.
Zhao, Y., Qian, Y., Sun, Z., Shen, X., Cai, Y., Li, L., Wang, Z., 2021. Role of PI3K in the progression and regression of atherosclerosis. Front. Pharmacol. 12, 632378.
Zhao, Y., Zhuang, Y., Shi, Y., Xu, Z., Zhou, C., Guo, L., Liu, P., Wu, C., Hu, R., Hu, G., Guo, X., Xu, L., 2021. Effects of N-acetyl-l-cysteine on heat stress-induced oxidative stress and inflammation in the hypothalamus of hens. J. Therm. Biol. 98, 102927.
Zhou, B., Xia, X., Wang, P., Chen, S., Yu, C., Huang, R., Zhang, R., Wang, Y., Lu, L., Yuan, F., Tian, Y., Fan, Y., Zhang, X., Shu, Y., Zhang, S., Bai, D., Wu, L., Xu, H., Yang, L., 2018. Induction and amelioration of methotrexate-induced gastrointestinal toxicity are related to immune response and gut microbiota. EBioMedicine 33, 122–133.